Radial Scattering of a Laser Beam in Anisotropic Scattering Media

H. F. Nelson* and B. V. Satish†
University of Missouri-Rolla, Rolla, Missouri

Experimental and theoretical results are compared for radiation scattered radially from a laser beam in an anisotropic scattering medium. An azimuthally symmetric He-Ne laser beam with Gaussian radial intensity distribution was incident normal to, and at the center of the top surface of, a scattering medium. The bottom and side surfaces of the cylinder containing the scattering medium were black. The scattering medium was composed of double-distilled water and spherical latex particles of uniform size. Radially scattered radiation was measured as a function of depth for two cases: 1) Rayleigh scattering and 2) strong forward anisotropic (Mie) scattering in the single scattering regime. The experimental data compare very well with the theoretical predictions. It is shown that the single scattering approximation holds for optical depths up to 0.4 for scattering media with depth-to-diameter ratios of unity.

Nomenclature

A = cross-sectional area of the detector slit
c = effective scattering coefficient, $6C_{sca}/(\pi d^3)$
C_{sca} = scattering cross section
d = diameter of the scattering particles
D = diameter of scattering medium, 9.5 cm
g = asymmetry factor
h = slit height, 0.38 cm
I^+ = intensity incident on the medium
I_i = intensity magnitude of the laser beam
I_{exp} = experimentally measured intensity leaving medium radially
I_r^+ = radially scattered intensity
I_a = intensity measured in air
I_m = intensity in medium
K = watt/volt conversion factor
ℓ = distance from center of laser beam to detector
L = depth of scattering medium, 9.5 cm
n = refractive index of the medium, 1.33
N = particle number density
P, P_i = detected and incident power, respectively
P_{90} = magnitude of phase function at 90 deg
r = radial distance from center of laser beam
r_o = effective radius of laser beam, 0.10 cm
R = radius of scattering medium, 4.75 cm
V = measured voltage
w = slit width, 0.10 cm
x = particle size parameter, $\pi dn/\lambda_0$
z = depth into the medium normal to top surface
β = extinction coefficient, $\eta c + \kappa$
$\delta(x)$ = Dirac delta function
$\Delta\Omega$ = incremental solid angle
η = particle volume concentration, $N\pi d^3/6$
θ = polar angle used to specify the direction of intensity
κ = absorption coefficient
λ_o = laser beam wavelength in air, 0.6328 μm
μ = $\cos\theta$
σ = scattering coefficient
τ_r = radial optical coordinate, βr
τ_{r_o} = laser optical radius, βr_o
τ_R = optical radius of scattering medium, βR
τ_z = depth optical coordinate, βz
τ_o = optical depth of scattering medium, βL
ϕ = azimuthal angle, used to specify the direction of the intensity, measured between the projection of the intensity on the r-ψ plane and the r axis
ω = single scattering albedo, σ/β

Received Aug. 1, 1986; revision received May 30, 1987.

*Professor of Aerospace Engineering, Department of Mechanical and Aerospace Engineering, Thermal Radiation Transfer Group. Associate Fellow AIAA.

†Graduate Student, Department of Mechanical and Aerospace Engineering, Thermal Radiation Transfer Group.

Introduction

SCATTERING of radiation in the radial direction from a cylindrical radiation source (i.e., laser beam) occurs in many practical situations. It has potential application in underwater visibility, medicine, and defense technology.

Stockham and Love[1] used a Monte Carlo method to investigate thermal radiation to the exterior base region of a finite cylindrical dispersion of absorbing, emitting, and anisotropically scattering particles. This problem was motivated by attempts to predict the base heating of a rocket caused by its exhaust plume.

Currently, there is considerable interest in the infrared radiation emission from missile plumes.[2,3] This situation involves scattering because the plumes typically contain aluminum oxide or carbon particles. The magnitude of the plume infrared signature in the broadside direction is very sensitive to the loading and size of the particles. In rocket plumes, emission is the source of the radiation.

Drop size and drop concentration in sprays have been measured by sideward laser light scattering.[4] Laser Doppler anemometer measurements rely on laser light scattering at typical backscatter angles of 30 deg from the beam axis.[5] Combustion processes have been analyzed by measuring the radially scattered intensity of a laser beam passing through the flame zone.[6,7]

The need for high-resolution nonintrusive methods to obtain quantitative information on mixing in turbulent flow has led to the development of light-scattering techniques to determine the molecular concentration and temperature profiles. The study of turbulent eddies and their relation to the large vortical structures developed upstream in the transition region of a jet requires fine temporal and spatial resolution and the simultaneous probing of an entire flow region.

Mie and Rayleigh scattering from a sheet of laser light have been used to measure the gas concentration field in aerosol-seeded turbulent jets.[8,9] The variation in the normally scattered light intensity from the light sheet is proportional to the gas concentration. Laser Raman scattering has been used in the experimental analysis of temperature and specie concen-

tration in an ionizing gas.[10] A high-power Q-switched ruby laser was used as a source of energy, and the Raman scattering was measured at 90 deg to the laser beam.

This paper presents a comparison of experimental data and theoretical calculations for radiation scattered radially from a laser beam. The laser beam propagates axially along the centerline of a cylindrically symmetric scattering medium, as shown schematically in Fig. 1. The radiation scattered radially out the sides of the scattering medium is measured as a function of distance along the cylinder. The scattering media are uniformally sized polystyrene latex spheres immersed in double-distilled water. The results presented here are for the single scattering regime.

The important parameters for experimental investigations involving two-dimensional scattering are albedo, optical depth, optical radius, and particle size parameter, ω, τ_o, τ_r, and x, respectively. The single scattering albedo is the ratio of scattering to extinction. When it is small, the medium is strongly absorbing, and when it is close to 1, the medium is almost pure scattering. The optical depth of the medium, τ_o, is a measure of the mean free path of photon travel in the z direction. It is controlled by the size and number density of scattering particles in the medium. In this study, polystyrene latex particles with diameters of 0.091 and 0.481 μm were used for scattering centers. Different concentrations of latex particles were used to obtain optical depths between 0.05 and 2.4. The optical radius of the medium, τ_R, is a measure of mean free path of photon travel in the radial direction and, for these experiments, is directly related to τ_o. τ_R varied from 0.025 to 1.2.

The particle size parameter x is the dimensionless ratio of the scattering particle circumference and the wavelength of the incident radiation. It can be used to classify the type of scattering. Mie theory gives the exact solution for scattering by an arbitrary homogeneous sphere. In the limit of vanishingly small x, Mie theory yields the Rayleigh theory solution as a limiting approximation. For x less than about 0.3, Rayleigh theory is a reasonably good approximation. For x greater than about 0.3, Mie theory must be used for the scattering solution. As x gets larger (of the order of 20), the Mie solution converges very slowly, and the principles of geometric optics are often used to obtain the scattering function. As x increases from 0.3, the scattering phase function becomes progressively more sharply peaked in the forward direction. The present investigation presents data for two suspensions of particles. In one, the particles are sufficiently small, compared to the wavelength, for Rayleigh theory to give good approximation. In the other, the particles are sufficiently large to require Mie theory.

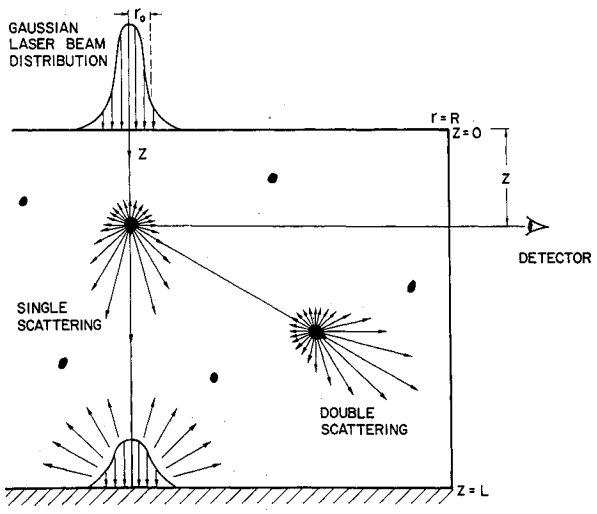

Fig. 1 Schematic of the physical situation. The laser beam is incident along the centerline axis of a right cylindrical scattering medium.

Theoretical Analysis

The theoretical development is based on the following assumptions: 1) steady state, 2) elastic scattering, 3) negligible interference and polarization effects, 4) homogeneous medium, 5) no emission, and 6) a two-dimensional, finite-depth, finite-radius scattering medium. The incident laser intensity is assumed to be collimated and normal to the surface of the scattering medium, as shown in Fig. 1. It can be expressed as

$$I^+ = I_i \delta(\mu - 1)\delta(\phi - 0)\exp[-(\tau_r/\tau_{r_o})^2] \tag{1}$$

where τ_r and τ_{r_o} are expressed as

$$\tau_r = (NC_{\text{sca}} + \kappa)r = (\sigma + \kappa)r = \beta r \tag{2a}$$

$$\tau_{r_o} = (NC_{\text{sca}} + \kappa)r_o = (\sigma + \kappa)r_o = \beta r_o \tag{2b}$$

The theoretical expression for the intensity scattered from a laser beam in the radial direction as it propagates through a scattering medium has been developed by Crosbie and Farrell.[11-13] The side-scattered intensity is

$$I_r^+(\tau_R, \tau_z) = \int_{-\tau_R}^{\tau_R} S(t, \tau_z)\exp[-(\tau_R - t)]\,dt \tag{3}$$

in which the loading is radially symmetrical, so that the source function $S(t, \tau_z)$ is not a function of angular location and t is a dummy variable representing radial optical depth. Following Refs. 11-13, the intensity in the radial direction becomes

$$I_r^+(\tau_R, \tau_z) = \frac{\omega}{4\pi}\exp(-\tau_z) I_i \int_0^{\tau_R} \exp[-(t/\tau_{r_o})^2] \times \{\exp[-\tau_R - t] + \exp[-\tau_R + t]\}\,dt \tag{4}$$

for single scattering of a laser beam with a Gaussian radial profile. Equation (4) can be integrated analytically to yield

$$I_r^+(\tau_R, \tau_z) = \frac{\omega}{4\sqrt{\pi}}\tau_{r_o} \times I_i \exp(-\tau_z)\exp(-\tau_R)\exp[(\tau_{r_o}/2)^2] \tag{5}$$

when $\tau_{r_o} \ll \tau_R$.

This result is for isotropic scattering. For optically thin, single scattering situations, Eq. (5) can be multiplied by the value of the normalized phase function at 90 deg, P_{90}, to account for anisotropic scattering. Equation (5) relates the radically scattered intensity inside the scattering medium to the incident intensity. To measure this intensity experimentally, the detector probe was located outside the glass tank containing the scattering medium. Thus, the radiation had to pass through the glass wall of the tank before it was detected. Consequently, refraction at the interface had to be accounted for. An energy balance across the interface yields[14]

$$I_a = I_r^+/n^2 \tag{6}$$

Therefore, the nondimensional intensity outside the glass wall is

$$\frac{I_a}{I_i} = \frac{I_r^+}{n^2 I_i} = \frac{\sigma}{4\sqrt{\pi}}\frac{r_o}{n^2}\exp[(\beta r_o/2)^2] \times \exp[-\tau_z]\exp[-\tau_R]P_{90} \tag{7}$$

in which the thickness of the glass walls has been ignored and where τ_R and τ_z contain the radial and depth variation. Note that I_a/I_i is directly proportional to $\sigma(=\omega\beta)$ and that it decreases linearly with τ_R and τ_z (R and z) for optically thin cases while, for larger optical depths, it decreases exponentially. In the limit as the optical thickness goes to zero, $\exp(-\tau_R) \simeq 1$, $\exp(-\tau_z) \simeq 1$, and $\exp[(\beta r_o/2)^2] \simeq 1$, so that I_a/I_i can be expressed as

$$\frac{I_a}{I_i} = \frac{\sigma r_o}{4\sqrt{\pi n^2}} P_{90} \tag{8}$$

Thus, in the optically thin limit, for a given set of experimental parameters σ, r_o, n, and P_{90}, the theoretical radial scattered intensity does not vary with depth or radius in the scattering medium.

Experimental Procedure

The experimental situation is depicted schematically in Fig. 1, The source, a 50-mW He-Ne laser, was incident normal to the medium surface at the center of the 9.5-cm-diam cylindrical glass tank. The medium consisted of double-distilled water and scattering particles. A black plastic sheet was placed just inside the sides of the glass tank, to reduce internal specular reflection from the glass walls. A 1-cm-wide vertical slot was left open in the sheet to measure the radially scattered flux. The tank was also fitted with a black bottom. The plastic sheet and the bottom were sprayed with a highly absorbing, diffusely reflecting black paint with a reflectance of less than 2%. The black plastic sheet eliminated any measurable wall effects. The black bottom was used to make the experimental situation represent an infinitely deep tank in order to be compatible with the theoretical solution.

Latex particles with diameters of 0.091 or 0.481 μm were used as scattering centers (one size at a time). Specific amounts of latex solution containing 1% latex particles and 99% distilled water by volume were added to double-distilled water to create the scattering medium. The amount of latex solution was determined by weighing it before adding it to the scattering medium. The specific gravity of the latex solution was assumed to be unity. The particles were thoroughly mixed, and no settling or any other discernible time variations were detected. The volume of latex solutions added to the given volume of water determined the optical characteristics of the medium.

The assumptions made in the laboratory data reduction calculations are as follows: 1) the laser beam flux and the scattering medium do not fluctuate during the time period required to read and record the output voltages as a function of depth; 2) the scattering medium is symmetrical, homogeneous, and finite in depth; 3) single scattering; 4) no emission; and 5) latex particles are pure scatterers.

Detector System

The detector system consisted of a detector probe, an optical light tube, a photomultiplier tube (PMT), and a digital multimeter. The probe was a hollow cylinder with an inside radius of 0.19 cm and a length of 2.54 cm. The probe, painted flat black both inside and outside to reduce reflection, was used to reduce the solid angle over which the scattered radiation was detected. A 1-mm-wide, 3.8-mm-high vertical slit was attached to the front of the probe to reduce the solid angle further. This slit width corresponded to the laser beam effective radius. The probe was mounted on a vertical rail, so that its position relative to the top of the tank could be varied and accurately determined. Optical light tubes made of high-transmission glass was used to transmit the laser light from the probe aperture to the PMT. The PMT converted the light signals to voltages, which were read on a digital voltmeter. Further details of the detection system design are given in Refs. 15 and 16.

Table 1 Latex particle parameters

d, μm	0.091	0.481
c, 1/cm	845	22,983
g	0.068	0.809
x	0.601	3.178
P_{90}	0.755	0.055

Scattering Particles

The particles used as scattering centers were selected from those commercially available from Dow Chemical. The polystyrene latex particles were spherical and uniform in size. Particles of two sizes were used so that widely varying scattering phase functions could be investigated. The small Rayleigh scattering particles had a 0.091-μm diameter and a 0.0058-μm standard deviation, while the larger Mie scatterers had a 0.481-μm diam and a 0.0018-μm standard deviation. The relative index of refraction of the latex particles to water at λ_o was 1.197.

The normalized scattering phase functions of the 0.091- and 0.481-μm-diam particles immersed in water at λ_o were generated using Mie theory and are shown in Fig. 2. The 0.481-μm particle phase function shows strong forward scattering, while the 0.091-μm particle phase function corresponds closely to a Rayleigh scattering distribution. The values of the particle size parameters and asymmetry factors are given in Table 1. The value of x for the 0.091-μm particles indicates that they cannot be strictly classified as Rayleigh scatters. Note, from Fig. 2, that they scatter slightly more in the forward direction (0 deg) than in the backward direction (180 deg). An asymmetry factor value of 0 indicates isotropic scattering, while a value near 1 indicates very strong forward scattering.

The value of the phase function at 90 deg is of interest for radial scattering. The value of P_{90} can be obtained from Fig. 2 as 0.755 and 0.055 for the 0.091- and 0.481-μm-diam particles,

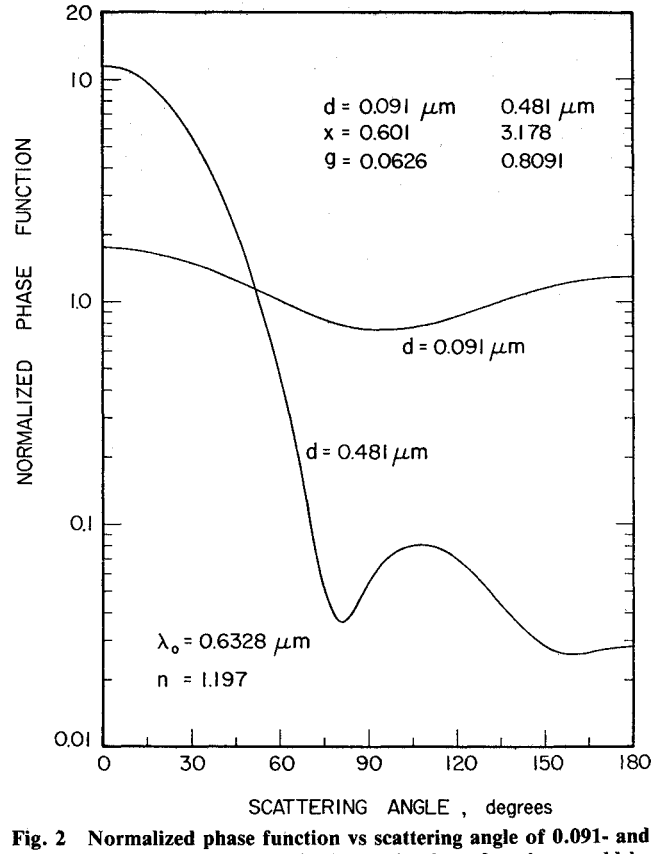

Fig. 2 Normalized phase function vs scattering angle of 0.091- and 0.481-μm-diam latex spheres. An isotropic phase function would be unity for all scattering angles.

respectively. Consequently, the 0.091-μm particles will exhibit more radial scattering than the 0.481-μm particles. The value of P_{90} for particles with an isotropic scattering phase function would be unity.

Data Analysis

The intensity of the scattered radiation received by the PMT is inversely proportional to the detector area and the solid angle and directly proportional to the detected power.

$$I_{\text{exp}} = P/(A\Delta\Omega) \tag{9}$$

The solid angle $\Delta\Omega$ is obtained by dividing the detection slit area by the distance from the laser beam to the detector squared, so that $\Delta\Omega = A/\ell^2 = hw/\ell^2$, because the detector slit area is hw. The length ℓ is the distance from the center of the laser beam to the near end of the detector probe, where the slit is attached. The front of the detector probe was 5.3 cm outside the glass wall for the 0.091-μm particle data ($\ell = 10.3$ cm) and 2.9 cm outside the glass wall for the 0.481-μm particle data ($\ell = 7.9$ cm). The actual power producing the intensity is related to the measured voltage. The conversion factor K (W/V) is gain-dependent and was determined from independent laboratory experiments. Thus, the detected power is linearly proportional to the measured voltage as $P = KV$, and Eq. (9) becomes

$$I_{\text{exp}} = KV[\ell/(hw)]^2 \tag{10}$$

The radial distribution of the incident laser beam intensity was Gaussian, so that the laser power incident on the medium obtained using Eq. (1) is[15,16]

$$P_i = 2\pi \int_0^{\infty} \left\{ \int_0^{2\pi} \int_0^{1} I^+(\tau_r, \mu, \phi)\mu \, d\mu \, d\phi \right\} r \, dr = \pi r_o^2 I_i \tag{11}$$

Thus, dividing Eq. (10) by I_i and using Eq. (11), one obtains

$$\frac{I_{\text{exp}}}{I_i} = \frac{\pi KV}{P_i}\left(\frac{\ell \, r_o}{wh}\right)^2 \tag{12}$$

in which $h = 0.38$ cm, $r_o = 0.10$ cm, $w = 0.10$ cm, and $\ell =$ either 7.9 cm or 10.3 cm. Equation (12) represents the experimental relation for the radially scattered intensity ratio. It is used to compare the experimental data to the theoretical solution as given by Eq. (7).

The optical thickness can be defined in terms of the particle volume concentration[15,16]

$$\eta = N\pi d^3/6 \tag{13}$$

From Eq. (2), the optical radius becomes

$$\tau_r = [\eta(6C_{\text{sca}}/\pi d^3) + \kappa]r = (\eta c + \kappa)r = \beta r \tag{14}$$

in which c is the effective scattering coefficient and, likewise, $\tau_{r_o} = \beta r_o$, $\tau_o = \beta L$, and $\tau_R = \beta R$. The value of κ for distilled water is 0.005 1/cm at $\lambda_0 = 0.6328$ μm.[15,16] The value of c for the latex particles was determined using Mie theory and is listed in Table 1.

Results and Discussion

This paper presents comparisons of experimental and theoretical results for radial scattering of a laser beam propagating through anistropic scattering media in the optically thin radius region for small to moderate optical depths. The radiation transfer is two-dimensional because the radiation enters the scattering medium in the z direction and is detected as it leaves in the r direction. The detected radiation is a function of both r and z (τ_r and τ_z). Data were obtained for an L/D ratio of unity, so that $\tau_R = \tau_o/2$. Scattering medium depth and diameter were both equal to 9.5 cm. Table 1 summarizes the particle parameters for the two sizes of latex particles used in the experiments. Table 2 gives the values of the experimental parameters.

Figures 3 and 4 show comparisons of the experimental and theoretical nondimensional radial scattered intensity as a function of depth below the upper surface of the scattering medium. The theoretical curves were obtained using Eq. (7). Figure 3 shows a comparison of experimental and theoretical results when the 0.091-μm-diam particles were used as scattering centers. The phase function at 90 deg for the 0.091 particles is 0.755, which implies that there is a large amount of radially scattered intensity. The agreement of the experimental and theoretical values of I_{exp}/I_i is good over the entire range of optical depths from 0.053 to 0.22, except near the tank bottom ($z = 9$). Reflection of the directly transmitted laser beam from the bottom causes the increase in the value of I_{exp}/I_i at small optical depths. Roughly 2% of the laser radiation reaching the bottom of the tank was diffusely reflected by the black plate at the bottom. When the detector probe was near the bottom, it began to collect some of this reflected radiation, even though it had a very small collection solid angle. In the optically thin cases, the reflected radiation completely masked the side-scattered radiation. However this occurs only very near the bottom and does not distort the majority of the data.

Figure 3 shows data near the optically thin limit. The experimental intensity does not vary with z at small values of τ_o. As τ_o increases, it begins to decrease faster with z or, in agreement with the theoretical predictions, τ_z.

Figure 4 shows a comparison between experimental and theoretical results at larger optical depths when the 0.481-μm-diam particles are used as scattering centers. The optical depth varied from 0.22 to 2.43. The phase function at 90 deg is 0.055. It is smaller than its corresponding value for the 0.091 particles, so that the 0.481 particles produce less radially scattered intensity than 0.091 particles for equal values of $\omega\tau_{r_o}$. This is predicted by Eq. (7) and is easily seen by comparing the ordinate values of Figs. 3 and 4 for the $\tau_o = 0.22$ cases. As in the preceding comparison for small optical depth cases, reflection of the directly transmitted laser beam from the bottom of the tank causes the detected radial intensity to increase near the bottom of the tank.

As the optical depth is increased, multiple scattering causes the difference between experiment and theory to increase. The breakdown of the single scattering assumption is the major cause of the poor agreement between the experiment and theory shown in Fig. 4 for optical depths greater than about 0.4. At $\tau_o = 2.426$, the theoretical solution and the experimen-

Table 2 Values of experimental parameters

$d = 0.091$ μm			
τ_o	τ_{r_o}	ω	σ(1/cm)
0.053	0.00055	0.097	0.00054
0.065	0.00069	0.270	0.00185
0.075	0.00079	0.367	0.00290
0.086	0.00090	0.445	0.00401
0.107	0.00113	0.557	0.00628
0.164	0.00173	0.711	0.0123
0.218	0.00230	0.782	0.0180
$d = 0.481$ μm			
τ_o	τ_{r_o}	ω	σ(1/cm)
0.220	0.00231	0.784	0.0181
0.258	0.00272	0.816	0.0222
0.322	0.00339	0.852	0.0289
0.386	0.00406	0.877	0.0356
0.482	0.00507	0.901	0.0457
2.426	0.0255	0.980	0.250

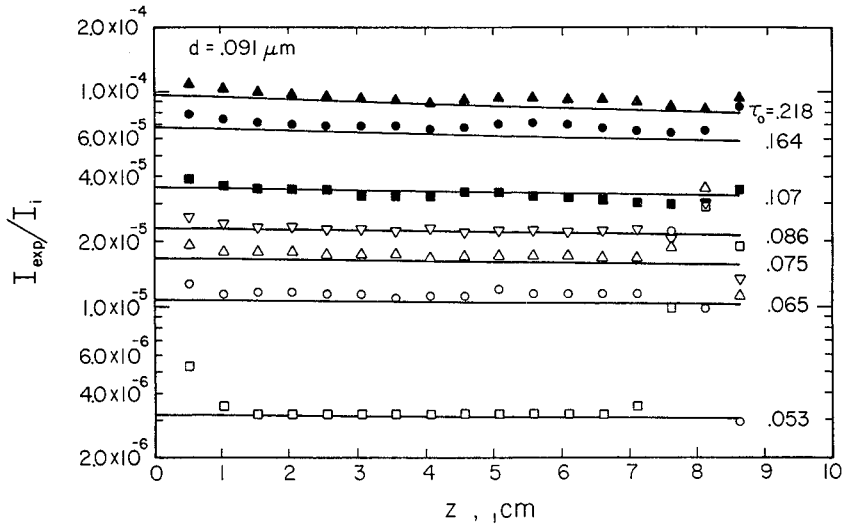

Fig. 3 Comparison of experimental (symbols) and theoretical (lines) results for side scattering as a function of depth for 0.091-μm particles for a range of optical depths ($L/D=1.0$; $\Delta\Omega=0.000361$ strad).

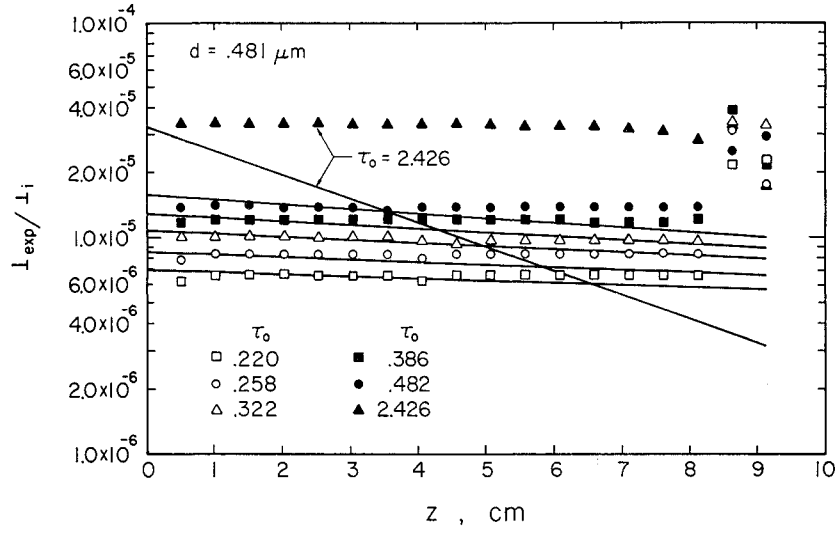

Fig. 4 Comparison of experimental (symbols) and theoretical (lines) results for side scattering as a function of depth for 0.481-μm particles for optical depths up to 2.43 ($L/D=1.0$; $\Delta\Omega=0.000610$ strad).

tal results behave differently. The value of I_{exp}/I_i does not drop very much as z increases, while the theoretical solution decreases considerably. The difference between the experimental and theoretical results is due to multiple scattering. Close inspection of Fig. 4 shows that multiple scattering effects begin to show up at values of τ_o as small as 0.25.

The theoretical solution implies that side-scattered intensity is directly proportional to the σ when τ_z and τ_R are small. The data presented in Figs. 3 and 4, together with the experimental parameters given in Table 2, confirm this result. Since σ ($=\eta c$) is directly related to η, it is very sensitive to the volume of latex particle solution used to make the scattering media. Small errors in the amount of latex particle solution and also in the dilutation of the 10% solution (as purchased) to 1% solution (as used) directly influence the side-scattered intensity.

Another possible source of error is in the alignment of the detector probe and the laser beam so that the detector probe moves directly along the beam. In our experimental setup, this was a very tedious adjustment and very hard to control. Alignment error could lead to systematic error trends, which could produce results such as those in Fig. 4 for $0.220<\tau_o<0.482$. In the future, this problem will be addressed.

It is important to note that this analysis does not use the effective optical coordinates as in Refs. 15 and 16. The effective optical coordinates account for the phase function model when multiple scattering is important.[17] In addition, the experimetnal data have been adjusted slightly to make the experiment and theory agree for the smallest τ_o case for the data shown in Figs. 3 and 4. This was done by multiplying Eq. (12) by a constant (very close to unity) to force the data to agree with the theory for the smallest τ_o case and then using the same value for the constant for all the other cases shown on the particular figure. This approach essentially compensated for possible errors in the magnitude of the parameters in Eq. (12).

Summary and Conclusions

The intensity that is radially scattered from a laser beam and transmitted through the sides of a cylindrical scattering medium was measured in the single scattering regime and compared to single scattering theory. An azimuthally symmetric He-Ne laser beam with a Gaussian radial intensity distribution was incident normal to, and at the center of, the top surface of the cylindrical scattering medium. The scattering medium consisted of double-distilled water and uniform-sized latex spheres. The bottom and sides of the scattering medium were black, except for a vertical slit approximately 1 cm in width, through which measurements were taken. The L/D ratio for the scattering medium was unity for all the mesurements.

Radiation transmitted through the sides of the scattering medium was measured as a function of depth from the top to the bottom of the tank. Experimental data were obtained for scattering particles with diameters of 0.091 and 0.481 μm. The optical depth was varied from 0.053 to 2.43.

Experimental results for optically thin media for I_{exp}/I_i as a function of depth compared very well with the single scattering theoretical results. At optical depths greater than 0.4, multiple scattering becomes important and the agreement between experiment and theory becomes poor. This occurs because of the breakdown of the single scattering assumption in the theoretical analysis. The very good agreement between the experiment and theoretical results in the optically thin regime shows the validity of the theoretical development. For scattering media with an L/D ratio of unity, the single scattering assumption holds for optical depths up to 0.4.

Acknowledgment

The authors acknowledge partial support of National Science Foundation Grants MEA 9121430 and CBT 8501099 for this research.

References

[1]Stockham, L.W. and Love, T.J., "Radiative Heat Transfer from a Cylindrical Cloud of Particles," *AIAA Journal,* Vol. 6, Oct. 1968, pp. 1935–1940.

[2]Nelson, H.F., "Influence of Particulates on Infrared Emission from Tactical Rocket Exhausts," *Journal of Spacecraft and Rockets,* Vol. 21, Sept.-Oct. 1984, pp. 425–432.

[3]Nelson, H.F., "Influence of Scattering on Infrared Signatures of Rocket Plumes," *Journal of Spacecraft and Rockets,* Vol. 21, Sept.-Oct. 1984, pp. 508–510.

[4]Beretta, F., Cavaliere, A., and D'Alessio, A., "Drop Size and Concentration in a Spray by Sideward Laser Light Scattering Measurements," *Combustion, Science and Technology,* Vol. 36, No. 1, 1984, pp. 19–37.

[5]Modarress, D., Tan, H., and Elghobashi, S., "Two-Component LDA Measurement in a Two-Phase Turbulent Jet, " *AIAA Journal,* Vol. 22, May 1984, pp. 624–630.

[6]"Laser Method Measures Soot Formation," *Laser and Applications,* Feb. 1985, pp. 38–40.

[7]Johnston, S.C., Dibble, R.W., Schefer, R.W., Ashurst, W.T., and Kollmann, W., "Laser Measurements and Stochastic Simulations of Turbulent Reacting Flows," *AIAA Journal,* Vol. 24, June 1986, pp. 918–937.

[8]Long, M.B., Chu, B.T., and Chang, R.K., "Instantaneous Two-Dimensional Gas Concentration Measurements by Light Scattering," *AIAA Journal,* Vol. 19, Sept. 1981, pp. 1151–1157.

[9]Escoda, M.C. and Long, M.B., "Rayleigh Scattering Measurements of the Gas Concentration Field in Turbulent Jets," *AIAA Journal,* Vol. 21, Jan. 1983, pp. 81–84.

[10]Galser, J.W. and Lederman, S., "Shock Tube Diagnostics Utilizing Laser Raman Scattering," *AIAA Journal,* Vol. 21, Jan. 1983, pp. 85–91.

[11]Farrell, J.B., "Multidimensional Scattering in Cylindrical Media," M.S. Thesis, Department of Mechanical and Aerospace Engineering, Univ. of Missouri-Rolla, 1981.

[12]Crosbie, A.L. and Farrell, J.B., "Exact Formulation of Multiple Scattering in a Three-Dimensional Cylinderical Geometry," *Journal of Quantitative Spectroscopy and Radiative Transfer,* Vol. 31, No. 5, 1984, pp. 397–416.

[13]Crosbie, A.L. and Farrell, J.B., "Multiple Scattering in a Two-Dimensional Finite Cylindrical Medium Exposed to a Laser Beam," *Journal of Quantitative Spectroscopy and Radiative Transfer* (to be published).

[14]Siegel, R. and Howell, J.R., *Thermal Radiation Heat Transfer,* 2nd ed., McGraw-Hill, New York, 1981, pp. 738–740.

[15]Look, D.C. Jr., Nelson, H.F. and Crosbie, A.L., "Anisotropic Two-Dimensional Scattering: Comparison of Experiment with Theory," *Journal of Heat Transfer,* Vol. 103, Feb. 1981, pp. 127–134.

[16]Nelson, H.F., Look, D.C. Jr., and Crosbie, A.L., "Two-Dimensional Radiative Back-Scattering from Optically Thick Media," *Journal of Heat Transfer,* Vol. 108, Aug. 1986, pp. 619–625.

[17]Crosbie, A.L., personal communication, May 1987.